THE JOURNAL OF PHYSICAL CHEMISTRY B

Article

Water Isotope Effect on the Phosphatidylcholine Bilayer Properties: A Molecular Dynamics Simulation Study

Tomasz Ro#g, Krzysztof Murzyn, Jeannine Milhaud, Mikko Karttunen, and Marta Pasenkiewicz-Gierula

J. Phys. Chem. B, **2009**, 113 (8), 2378-2387• DOI: 10.1021/jp8048235 • Publication Date (Web): 30 January 2009

Water Isotope Effect on the Phosphatidylcholine Bilayer Properties: A Molecular Dynamics Simulation Study

Tomasz Róg,[†,‡] Krzysztof Murzyn,[‡] Jeannine Milhaud,[§] Mikko Karttunen,[||] and Marta Pasenkiewicz-Gierula*[,‡]

Department of Physics, Tampere University of Technology, Tampere, Finland; Department of Biophysics, Faculty of Biochemistry, Biophysics and Biotechnology, Jagiellonian University, Kraków, Poland; Laboratoire de Biophysique Moléculaire, Cellulaire et Tissulaire, UFR SMBH Université Paris 13, Paris, France; and Department of Applied Mathematics, The University of Western Ontario, London, Ontario, Canada

Received: June 1, 2008; Revised Manuscript Received: December 1, 2008

Physicochemical properties of heavy water (D_2O) differ to some extent from those of normal water. Substituting D_2O for H_2O has been shown to affect the structural and dynamic properties of proteins, but studies of its effects on lipid bilayers are scarce. In this paper, the atomic level molecular dynamics (MD) simulation method was used to determine the effects of this substitution on the properties of a dipalmitoylphosphatidylcholine (DPPC) bilayer and its hydrating water. MD simulations of two DPPC bilayers, one fully hydrated with H_2O and the other with D_2O, were carried out for over 50 ns. For H_2O, the simple point charge (SPC) model was used, and for D_2O, the extended SPC-HW model was employed. Analyses of the simulation trajectories indicate that several properties of the membrane core and the membrane/water interface are affected by replacing H_2O by D_2O. However, the time-averaged properties, such as membrane compactness, acyl chain order, and numbers of PC−water H (D)-bonds and PC−PC water bridges, are much less affected than time-resolved properties. In particular, the lifetimes of these interactions are much longer for D_2O molecules than for H_2O ones. These longer lifetimes results in a slightly better ordering of the D_2O molecules and average self-diffusion, which is 50% slower compared with the H_2O molecules. This large isotope effect has been assigned to the repercussions of the longer lived D-bonding to DPPC headgroups insofar as all water molecules sense the presence of the DPPC bilayer.

Introduction

Vienna Standard Mean Ocean Water (VSMOW, recommended by IUPAC in "Atomic Weights of the Elements: Review 2000"), which represents the water content of earth, contains ∼0.015% deuterium (^{2}H, D) oxide (D_2O, heavy water); thus, D_2O constitutes only a fractional component of the water on earth. Heavy water, which can be separated from regular water by various chemical exchange processes, has somewhat different physicochemical properties than normal water.[1] Because of that, D_2O is often used as a solvent for biomolecules in nuclear magnetic resonance, neutron scattering, Raman, and Fourier transform infrared (FTIR) experiments. In those experiments, the effect of D_2O substitution for H_2O on biomolecules is considered to be small.

It is well-known, however, that macromolecules in contact with D_2O tend to reduce their surface area by adopting a globular shape or by aggregating.[2,3] D_2O has also an influence on cells and living organisms, though to a different extent. At concentrations higher than 20% of body weight, heavy water can be toxic to animals and animal cells[4] but not to prokaryotes, although their growth rate is affected.[5,6]

The effects of heavy water on biomolecules are often classified into two groups:[2] "solvent isotope effects" and "deuterium isotope effects". Solvent isotope effects arise mainly from the higher stability of the hydrogen bond network in liquid D_2O than that in liquid H_2O and from the different strengths of solute−solvent interactions in D_2O and in H_2O.[2] Ab initio calculations at the MP2 level show that the binding energy of a D_2O dimer is higher than that of a H_2O dimer, and this tendency becomes more pronounced when the size of the oligomer increases.[7] The more restricted atomic vibrations in D_2O reduce the negative effect of its van der Waals repulsion, thus increasing its binding energy via hydrogen bonds. Deuterium isotope effects result from the H/D isotopic exchange between biomolecules and heavy water.[2] This affects both intra- and intermolecular interactions as well as the rates of chemical reactions involving the biomolecules and thus alters their biological activity.

The effect of substituting D_2O for H_2O on the structure and dynamics of lipid aggregates, and especially phospholipid bilayers, is not fully recognized despite the fact that water molecules at the bilayer interface play a crucial role.[8,9] Experimental studies carried out so far have demonstrated that this substitution influences the interfacial region and affects the phase behavior of phosphatidylcholine (PC) bilayers.[10] Matsuki et al.[10] attributed these effects to the D_2O-induced decrease of the bilayer surface area; however, they did not provide the precise magnitude of the decrease. In another experimental study using mixed PC bilayers, Takuke et al.[11] indicated that D_2O restrains the mixing of phospholipids with saturated chains of different lengths. This result was attributed to tighter packing of bilayers hydrated with D_2O instead of H_2O and also due to the fact that D_2O penetrates the hydrocarbon core of a saturated PC bilayer less deeply than H_2O. In addition, experiments on

* To whom correspondence should be addressed: tel +48-12-664-6518; fax +48-12-664-6902; e-mail mpg@mol.uj.edu.pl.
[†] Tampere University of Technology.
[‡] Jagiellonian University.
[§] UFR SMBH Université Paris 13.
[||] The University of Western Ontario.

10.1021/jp8048235 CCC: $40.75
Published on Web 01/30/2009

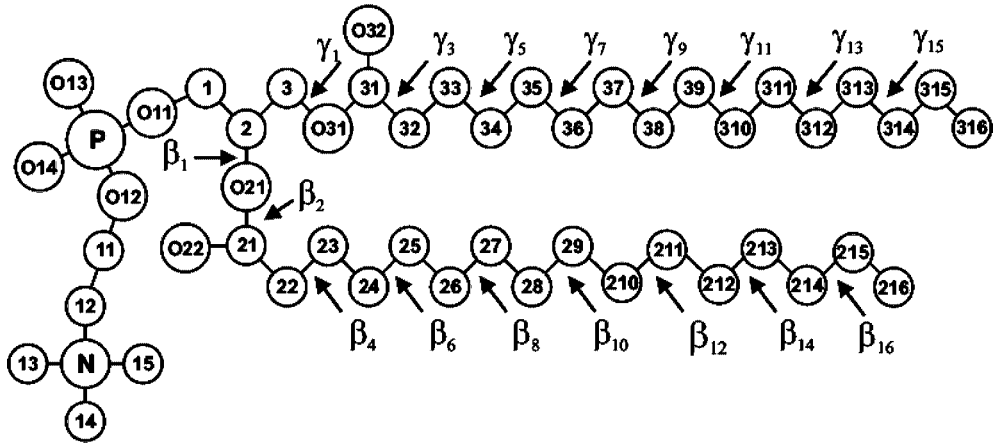

Figure 1. Molecular structure of DPPC with numbering of atoms and torsion angles. The chemical symbol for carbon atoms, C, and their attached H atoms have been omitted. The β- and γ-chain of DPPC are indicated.

PC/water/pyridine reverse micelles[12] have shown that micelles form dimers in the presence of D_2O but not in the presence of H_2O.

The molecular dynamics (MD) simulation method is a well-suited to study the complex dynamic behavior of molecules in relatively short time scales (up to about 100−200 ns). MD simulations of hydrated lipid bilayers have shown numerous but short-lived H-bonds between lipid headgroups and water molecules as well as an extended network of interlipid links via water molecules that are simultaneously H-bonded to two lipid molecules, i.e., so-called water bridges.[14,15] Recent experiments on a PC bilayer weakly hydrated in D_2O[15] have confirmed the MD simulation results that water molecules are involved in water bridging in addition to simple H (D)-bonding to PC polar groups. The dynamic character of lipid−water D- and H-bonds and water bridges was shown experimentally by Volkov et al.[15]

Computer simulation studies addressing the effects of water D for H isotopic substitution are scarce. The simplest approach in modeling the D_2O molecule is to double the mass of H in the water molecule. Such an approach was used in the study of pure water[16] and the effect of D_2O on plastocianine.[17] A more rigorous approach must include additional corrections to the partial charges on the hydrogen and oxygen atoms. Such D_2O models have been used to investigate the behavior of OH^- and OD^- in H_2O[18] and of pure D_2O[19] as well as in the present paper.

In this paper, we present the results of 50 ns MD simulations of dipalmitoylphosphatidylcholine (DPPC) bilayers hydrated with H_2O and D_2O. We address the following questions that are of experimental relevance: (1) what is the effect of D_2O on bilayer properties such as membrane compactness, water penetration, and chain order, (2) what is the effect of D_2O on the PC−PC interactions in the bilayer interfacial region, and (3) what are the properties of D_2O and H_2O molecules at the bilayer interface?

Methods

System Description and Parameters. Atomic-scale molecular dynamics (MD) simulations of two membrane systems composed of 128 DPPC molecules were performed. The first bilayer was hydrated with 3650 H_2O molecules (DPPC−H_2O) and the second with the same number of D_2O molecules (DPPC−D_2O). The initial structure of both bilayers was the final structure of our previous 100 ns DPPC simulation.[20] The bilayers were simulated for over 50 ns using the GROMACS software package.[21] Figure 1 shows the structure, the numbering of atoms, and the torsion angles in the DPPC molecule.

TABLE 1: Numerical Values of Force-Field Parameters for ESP H_2O and ESP-HW D_2O[a]

parameter	H_2O	D_2O
H−O bond length [nm]	0.1	0.1
bond H−O force constant [kJ/mol]	345000	345000
H−O−H valence angle [deg]	109	109
angle H−O−H force constant [kJ/mol]	383	383
vdW oxygen r^*	0.26171E−02	0.26171E−02
vdW oxygen ε	0.26331E−05	0.26331E−05
vdW hydrogen r^*	0.00000E+00	0.00000E+00
vdW hydrogen ε	0.00000E+00	0.00000E+00
partial charge on oxygen	−0.8476	−0.870
partial charge on hydrogen/deuterium	0.4238	0.435
oxygen mass [aum]	16	16
hydrogen mass [aum]	1	2

[a] r^* and ε are the van der Waals (vdW) radius and well depth, respectively. Partial charges are in electrostatic units.

We used standard united atom force-field parameters for DPPC molecules,[22] where the partial charges were taken from the underlying model description.[23] For H_2O, the SPC (simple point charge) model was employed.[24] For D_2O, the SPC-HW model (HW = heavy water), tested successfully in a pure water simulation,[19] was used. In this model, the mass of D is twice the mass of H. The bonding and the van der Waals parameters are the same as for H_2O, and the partial charges on O and D atoms are scaled to account for the larger effective dipole moment of D_2O; the dipole moment of D_2O is 3% larger than that of H_2O.[19] The force-field parameters for H_2O and D_2O are given in Table 1.

The LINCS algorithm[25] was used to preserve the lengths of the O−H and O−D bonds, and the time step was set to 2 fs. Periodic boundary conditions were used in all directions. The van der Waals (vdW) interactions were cut off at 1.0 nm, and the electrostatic interactions were evaluated using the particle-mesh Ewald (PME) summation.[26] A real space cutoff of 1.0 nm with the usual minimum image convention, β spline interpolation order of 5, and direct sum tolerance of 10^{-6} were used. The simulation protocol used in this study has been successfully applied in various MD simulation studies of lipid bilayers.[20,27]

The MD simulations were carried out in the *NPT* ensemble (constant particle number, pressure, and temperature), at a pressure of 1 atm and temperature of 323 K, which is above the main phase transition temperature of DPPC.[28] The temper-

atures of the solute and solvent were controlled independently. Both temperature and pressure were controlled by the weak coupling method[29] with the relaxation times set to 0.6 and 1.0 ps, respectively. Pressure was controlled semi-isotropically.

Analyses. In the analyses below, various quantities were determined from the trajectories generated in MD simulations of the DPPC−H_2O and DPPC−D_2O bilayers. The surface area/DPPC was calculated by dividing the total area of the membrane by 64, which is the number of DPPC molecules present in each leaflet. The membrane thickness was estimated from the mass density profiles by using two slightly different definitions: first by considering the points where the mass densities of lipids and water are equal[27] and second from the mass densities of lipids and water at a given bilayer depth by using the equation

$$d = \int \frac{\rho_{\text{lipid}}}{\rho_{\text{lipid}} + \rho_{\text{water}}} \, \mathrm{d}z \qquad (1)$$

where ρ_{lipid} and ρ_{water} are the local mass densities of the lipids and water at depth z, respectively, and z is the bilayer depth along the normal.[30] When averaging conformation-related quantities, only the torsion angles 4−16 (see Figure 1) were taken into account since, as was shown in the case of DMPC bilayers,[31] the torsion angles $\beta 3$ and $\gamma 3$ are not in well-defined, stable conformations (*trans* or *gauche*). The tilt angle of an acyl chain was measured using $\arccos((\langle \cos^2 \theta \rangle^{1/2}))$, where θ is the angle between the bilayer normal and the average segmental vector (averaged over the appropriate segmental vectors ≥4), and $\langle ... \rangle$ denotes both the ensemble and the time averages. The nth segmental vector, i.e., the (C_{n-1}, C_{n+1}) vector, links the (n − 1)th and the (n + 1)th C atoms along the acyl chain.[32] To analyze hydrogen bonding, water bridging, and charge pairing, the same geometrical definitions as in our previous papers were employed.[14,15] A H-bond between an OH group of a water molecule and an oxygen atom of PC or water molecules is judged to be formed when the O···O distance (r) is <3.25 Å and the angle between the O···O vector and the OH bond (the O···O−H angle) is <35°; a water bridge consists of a water molecule that is simultaneously H-bonded to two lipid oxygen atoms. A charge pair is formed between a positively charged choline methyl group (N−CH_3) and negatively charged non-ester phosphate or carbonyl oxygen atom when they are located within 4.0 Å from each other.

Results

Characteristic of the Membrane System. *Equilibration.* Equilibration was determined by monitoring the timed development of temperature (no data shown), potential energy (Figure 2a), and the area per lipid (Figure 2b). It was concluded from those profiles that the DPPC−D_2O bilayer is near equilibrium very shortly after the start of the simulation. This is not surprising since only very minor changes were introduced into the system, which was previously simulated for 100 ns.[20] Nevertheless, in all the analyses below, the first 5 ns fragment of each trajectory was treated as an equilibration period, and hence discarded, and the remaining 45 ns was used in the analyses.

Surface Area and Membrane Thickness. When water is deuterated, the average surface area/DPPC is about 2% smaller than when it is not; the detailed values are given in Table 2. This difference is comparable to the standard deviation (SD), but it is larger than the standard error (SE) estimate equal to SD/$n^{1/2}$, where n, the number of independent observations, is only five.

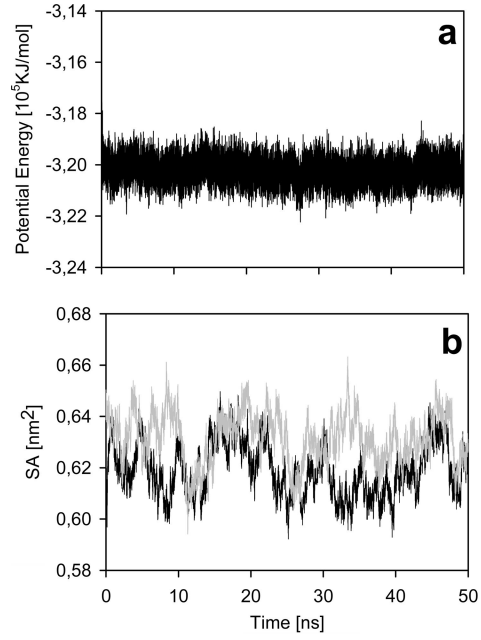

Figure 2. Time profiles of the (a) potential energy and (b) the surface area per DPPC in the DPPC−D_2O bilayer (black line). Additionally, (b) the time profile of the surface area per DPPC in the DPPC−H_2O bilayer (gray line) is plotted.

TABLE 2: Parameters Characterizing the DPPC Bilayer[a]

membrane		DPPC−H_2O	DPPC−D_2O
S_{mol}	β-chain	0.318 ± 0.005	0.334 ± 0.005
	γ-chain	0.330 ± 0.005	0.349 ± 0.005
tilt (deg)	β-chain	22.2 ± 0.5	21.7 ± 0.5
	γ-chain	22.7 ± 0.5	22.1 ± 0.5
no. *gauche*	β-chain	2.73 ± 0.03	2.70 ± 0.03
	γ-chain	2.76 ± 0.03	2.73 ± 0.03
lifetime (ps)	β-chain	87 ± 2	89 ± 2
	γ-chain	85 ± 2	87 ± 2
no. of neighbors	β-chain	33.68 ± 0.05	34.05 ± 0.05
	γ-chain	34.16 ± 0.05	34.53 ± 0.05
area/DPPC [nm^2]		0.631 ± 0.006	0.619 ± 0.006
thickness [nm]		4.15/3.75 ± 0.01	4.15/4.01 ± 0.01
$D \times 10^{-5}$ [cm^2/s]		2.58 ± 0.06	1.48 ± 0.06

[a] Average values of the molecular order parameter, S_{mol}, chain tilt angle, number of *gauche* conformations per acyl chain, lifetimes of *trans* conformations, and number of neighbors for the β- and γ-chain atoms of DPPC. Also given are the average surface area per DPPC and the membrane thickness calculated by the two methods cited in the Analyses section as well as the diffusion coefficients of H_2O and D_2O for DPPC−H_2O and DPPC−D_2O bilayers. Errors in the average values are standard deviation estimates, except for the area/DPPC, where errors are standard error estimates.

Because of limited compressibility of a PC bilayer, a decrease of the surface area is associated with an increase in membrane thickness. Membrane thickness is not a well-defined quantity, and its value may depend on the way it is calculated. The thickness of DPPC−H_2O and DPPC−D_2O bilayers, calculated from the partial density profiles (Figure 3) by the first method[27] described in the Analyses section, is 4.1 nm for both bilayers. Using the second method[30] (see Analyses section), the values are 3.75 and 4.01 nm for the DPPC−H_2O and DPPC−D_2O bilayer, respectively. It can be seen from Figure 3 that substituting D_2O for H_2O affects the mass density profile—in the DPPC−D_2O bilayer the partial density along the bilayer normal in the headgroup region is higher and in the bilayer center lower than those in the DPPC−H_2O bilayer. In addition, D_2O penetrates the bilayer slightly less deeply than H_2O. These

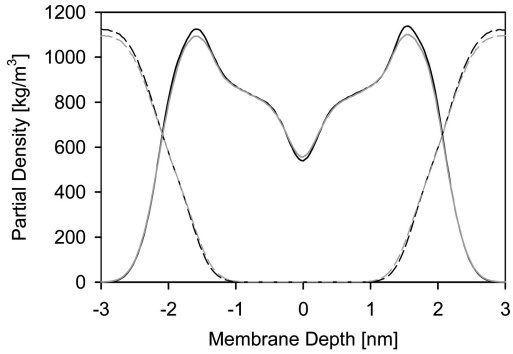

Figure 3. Partial density profiles along the bilayer normal of DPPC (solid line) and water (dotted line) in DPPC−H_2O (gray line) and DPPC−D_2O (black line) bilayers. The coordinate $z = 0$ corresponds to the membrane center.

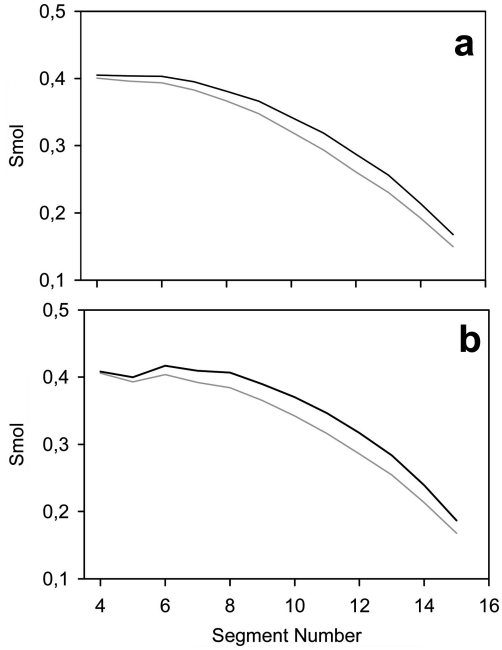

Figure 4. Profiles of the molecular order parameter (S_{mol}) calculated for (a) the DPPC β-chain and (b) γ-chain in DPPC−H_2O (gray line) and DPPC−D_2O (black line) bilayers. An average error (standard deviation estimate) is 0.005.

results cannot be quantitatively compared to experimental data due to the lack of precise experimental values.

Bilayer Core. ***Order and Conformation of Acyl Chains.*** Substitution of H_2O by D_2O as the membrane hydrating water causes a measurable increase of the order of the DPPC acyl chains. The molecular order parameter, S_{mol}, is used to characterize the order of acyl chains in membranes. For the nth segment, S_{mol} is defined as

$$S_{mol} = \frac{1}{2}\langle 3\cos^2\theta_n - 1\rangle \qquad (2)$$

where θ_n is an instantaneous angle between the nth segmental vector (see Analyses section) and the bilayer normal; $\langle ... \rangle$ denotes both the ensemble and the time averages.[33,34] S_{mol} profiles along the β- and γ-chain of DPPC are shown in Figure 4. The mean values of S_{mol} as well as the tilt angle, the number of *gauche* conformations per chain, and the lifetime of the *trans* conformation are given in Table 2. The slight increase in the order of acyl chains due to the isotopic exchange may be due to a decrease of the chain tilt angle and an increase in the *trans* conformation lifetime. These changes are, however, small, and they are consistent with the observed smaller surface area per PC in the DPPC−D_2O bilayer as compared with the DPPC−H_2O one.

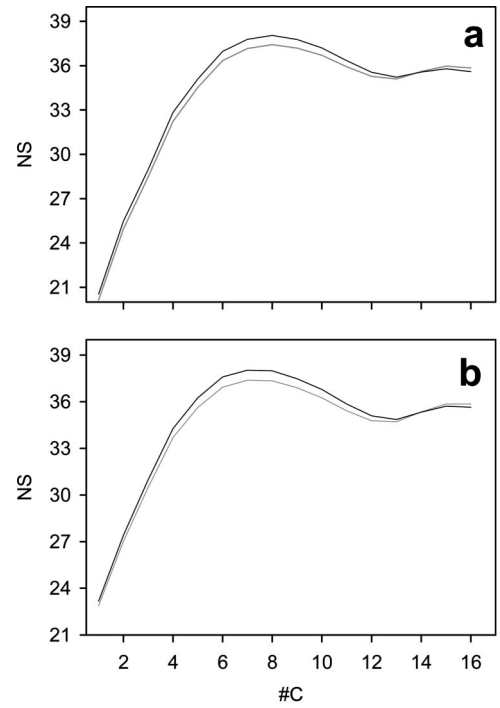

Figure 5. Profiles of the number of neighbors (NS) along (a) the β-chain and (b) the γ-chain in DPPC−H_2O (gray line) and DPPC−D_2O (black line) bilayers. An average error (standard deviation estimate) is 0.05.

Packing of Atoms. The packing of atoms in the bilayer core can be estimated by calculating the average number of neighbors using the method described in refs 35 and 36. The neighbor of an arbitrarily chosen carbon atom in the bilayer core is an atom belonging to a different molecule and located no further than 0.7 nm from the carbon atom in question. The distance 0.7 nm is the position of the first minimum in the carbon−carbon radial distribution functions (RDF).[35] The average number of neighbors was 33.92 ± 0.05 in the DPPC−H_2O bilayer and 34.29 ± 0.05 in the DPPC−D_2O one (Table 2). The difference in these values is small but is statistically significant. Profiles showing the numbers of neighbors along the β- and γ-chains are given in Figure 5.

Membrane/Water Interface. ***Headgroup−Water Interactions.*** In the following, we call the non-ester phosphate oxygen atoms (O13 and O14, Figure 1) collectively as Op, the carbonyl oxygen atoms (O22 and O32, Figure 1) as Oc, and the water oxygen as Ow. Figure 6 shows the RDFs of the Ow atoms relative to choline carbon, Op, O22, and O32 atoms in DPPC−H_2O and DPPC−D_2O bilayers. The shapes of RDFs for both systems are similar. Their extremal values, however, differ slightly, indicating subtle differences in the geometry of the headgroup−water H-bonds compared with D-bonds; distributions of the H-bond distances and angles (data not shown) indicate that for D-bonds the distance and angle are smaller than for H-bonds. It should be noticed, however, that similarly to the observations by Nemethy and Scheraga,[37] the average values are not statistically different (Table 3). Thus, for both systems, we applied the same geometric definitions of H-bonding and water bridging as well as water forming clathrate-like structures around choline groups (see Analyses section).

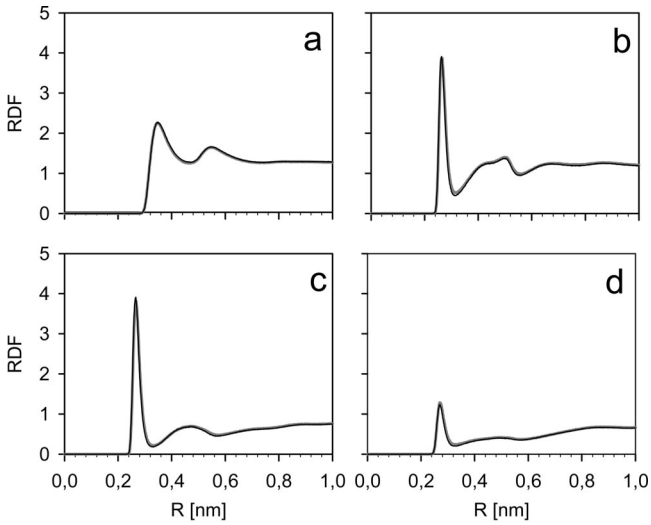

Figure 6. Radial distribution functions (RDF) of the water oxygen atoms relative to (a) choline carbon atoms, (b) phosphate oxygen (O13 and O14) atoms, and carbonyl oxygen (c) O22 and (d) O32 atoms in DPPC−H_2O (gray line) and DPPC−D_2O (black line) bilayers.

TABLE 3: Interactions in the Membrane/Water Interface[a]

	DPPC−H_2O	DPPC−D_2O
H-bonds	6.0 ± 0.34	5.8 ± 0.32
H-bonded water	5.5	5.3
bridges	1.1	1.1
choline water	7.56 ± 0.24	7.77 ± 0.25
anchoring water	4.38 ± 0.13	4.34 ± 0.13
charge pairs	2.6	2.6
R_{Hb} [nm]	0.272 ± 0.016	0.271 ± 0.016
θ_{Hb} [deg]	11.64 ± 6.42	11.33 ± 6.28

[a] Average numbers of PC−H_2O and PC−D_2O H-bonds, water molecules H-bonded to PC, water bridges, water molecules in a clathrate around the choline group (choline water), anchoring water molecules (anchoring water), and charge pairs in DPPC−H_2O and DPPC−D_2O bilayers. Average values for the H-bond and D-bond distance (R_{Hb} = Op···O) and the H-bond and D-bond angle (θ_{Hb} = Op···O−H (D)) for water···Op H-bond in DPPC−H_2O and DPPC−D_2O bilayers are also given. Errors in the average values are standard deviation estimates; for water bridges and charge pairs they are smaller than 0.04.

TABLE 4: Interactions in the Membrane/Water Interface[a]

oxygen	DPPC−H_2O	DPPC−D_2O
O14	1.53 ± 0.05	1.51 ± 0.05
O13	1.54 ± 0.05	1.49 ± 0.05
O22	1.55 ± 0.05	1.53 ± 0.05
O32	0.58 ± 0.05	0.54 ± 0.04
O12	0.41 ± 0.04	0.40 ± 0.04
O11	0.13 ± 0.03	0.12 ± 0.03
O21	0.18 ± 0.054	0.17 ± 0.03
O31	0.06 ± 0.02	0.06 ± 0.02
total	6.0 ± 0.34	5.8 ± 0.32

[a] Average numbers of direct H bonds between water and PC oxygen atoms: non-ester phosphate O14 and O13, carbonyl O22 and O32, ester phosphate O12 and O11, and glycerol O21 and O31 (cf. Figure 1) in DPPC−H_2O and DPPC−D_2O bilayers. Errors in the average values are standard deviation estimates.

For all DPPC oxygen atoms, the number of H-bonds with H_2O, as well as the number of H-bonded H_2O molecules per DPPC (Tables 3 and 4), is ∼4% higher than in the case of D_2O (Tables 3 and 4). The number of solvent molecules in a clathrate around the choline group is ∼3% higher in the case of D_2O than in the case of H_2O (Table 3). A more detailed discussion concerning the number of water molecules H-bonded to the carbonyl oxygen atom O22 is provided in the Discussion section.

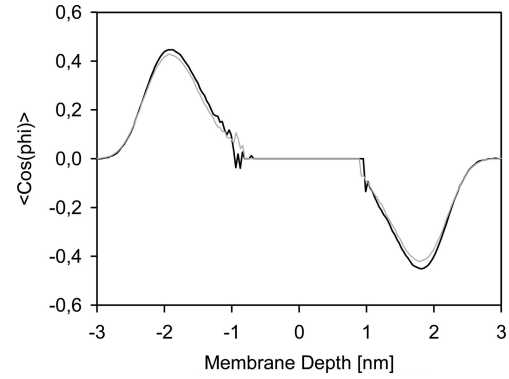

Figure 7. Orientation of water molecules characterized by an average cosine of the angle between the water dipole and the bilayer normal in DPPC−H_2O (gray line) and DPPC−D_2O (black line) bilayers.

Water Bridging. The number of water molecules that are simultaneously H-bonded to two DPPC molecules (water bridges) is 1.1/DPPC in both DPPC−H_2O and DPPC−D_2O bilayers (Table 3). However, the percentage of H-bonded water molecules engaged in bridging is higher in the DPPC−D_2O bilayer (Table 3) because the number of H-bonded water molecules per DPPC is smaller.

Water Anchoring. Our analysis indicates that some of the water molecules forming a clathrate around the choline group are simultaneously H-bonded to Op and Oc atoms of the same or another PC molecule. We call these linking water molecules "anchoring water" to distinguish them from bridging water. This analysis gives, for the first time, the number of anchoring water molecules per DPPC (Table 3). The number is practically the same in both bilayers and is unexpectedly high as anchoring water constitutes ∼57% of water molecules in the clathrate. Because an average number of water molecules in the clathrate is slightly larger in the DPPC−D_2O bilayer, the percentage of clathrating water molecules engaged in anchoring is ∼1% lower in the DPPC−D_2O than in the DPPC−H_2O bilayer (Table 3).

Charge Pairing. Substituting D_2O for H_2O does not change the number of charge pairs per DPPC: it is equal to 2.6 in both systems (Table 3).

Order and Dynamics of Water Molecules. ***Water Order.*** Ordering of water molecules in the vicinity of the membrane/water interface can be characterized by the time averaged projection, $P(z)$, of the water dipole unit vector $\boldsymbol{\mu}(z)$ onto the interfacial normal, $\mathbf{n}$; $P(z) = \langle \boldsymbol{\mu}(z) \cdot \mathbf{n} \rangle = \langle \cos \varphi \rangle$,[30] where z is the vertical distance of the center-of-mass (CM) of the water molecule from the bilayer center, $\mathbf{n}$ is a unit vector pointing away from the bilayer center, and φ is the angle between $\boldsymbol{\mu}(z)$ and $\mathbf{n}$. The average orientation of the water dipole as a function of z in DPPC−H_2O and DPPC−D_2O bilayers differs slightly (Figure 7); D_2O dipoles are more aligned along the normal to interface than H_2O dipoles, and thus, in the interfacial region, D_2O molecules are slightly more ordered than H_2O ones. The distribution of angles φ is maximum (∼60°, see Figure 7) for the orientation of the dipole vector corresponding to a H (D)-bonding to the phosphate oxygen atoms.

Water Self-Diffusion. Mean-square displacement (MSD) curves for the CM of H_2O and D_2O molecules in the bilayers are shown in Figure 8. MSD is defined as

$$\mathrm{MSD}(\tau) = \langle |r(t_0) - r(t_0 + \tau)|^2 \rangle_{t_0} \qquad (3)$$

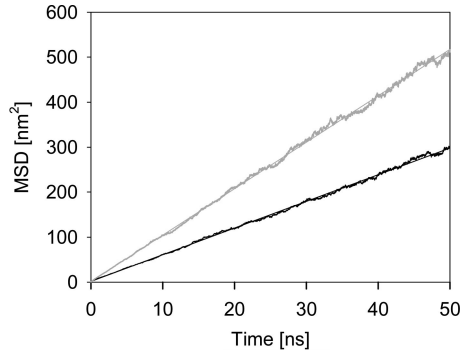

Figure 8. Mean-square displacement (MSD) of all water molecules in DPPC−H_2O (gray line) and DPPC−D_2O (black line) bilayers.

where r is the position of the molecule's CM, t_0 and τ are the initial and measurement times, respectively, and $\langle ... \rangle_{t_0}$ denotes an averaging over different initial time values within a simulation run and over all molecules in the system. Self-diffusion coefficients of H_2O and D_2O molecules (Table 2) averaged over all water molecules were calculated from the linear parts of the respective MSD curves. The self-diffusion coefficient of D_2O molecules (1.48×10^{-5} cm^2/s, Table 2) is reduced to almost half that of H_2O molecules (2.58×10^{-5} cm^2/s, Table 2). These values are smaller than those determined experimentally for bulk water at similar temperature, 3.54×10^{-5} and 4.46×10^{-5} cm^2/s for D_2O and H_2O, respectively.[38] The increase of the isotope effect from 21% to 43% in our systems clearly shows that the presence of the DPPC bilayer has a strong influence on the lateral diffusion of water molecules, particularly on D_2O.

Dynamics of PC−Water H-Bonds and PC−PC Charge Pairs. The dynamics of H-bonds between the water molecules and the DPPC headgroups in the interfacial region of the DPPC bilayer was analyzed using the hydrogen-bond time correlation functions, C_{HB},[39] defined as

$$C_{HB}(\tau) = \frac{\langle h_{wPC}(t_0) h_{wPC}(t_0 + \tau) \rangle}{\langle h_{wPC} \rangle} \quad (4)$$

In eq 4, $h_{wPC}(t)$ is unity when a particular water molecule and a particular DPPC headgroup are H-bonded at time t and zero otherwise. $\langle ... \rangle$ denotes averaging over all considered DPPC−water H-bonds and over initial time values t_0. Physically, C_{HB} represents the probability that the bond existing at $t = t_0$ still exists after a delay τ and allows for temporal breaks. Plots of time correlation functions for selected DPPC−water H-bonds (C_{HB}), for water bridges (C_{WB}), and for selected charge pairs (C_{CP}) as a function of τ for both bilayers are shown in Figure 9. C_{WB} and C_{CP} were calculated in the same way as C_{HB}.

In general, these decays involve different simultaneous processes, and hence the corresponding plots can be fitted to a sum of exponentials

$$C(t) = \sum_{i=1}^{N} A_i \exp(-t/T_i) \quad (5)$$

where T_i is the time constant and A_i the amplitude of the ith individual decay process and N is the number of exponentials. N is generally not known beforehand. Because of nonorthogonality of the exponentials, unambiguous determination of the proper values for T_i, A_i, and N is not easy.[40] To determine their values, we carried out several tests which showed that four

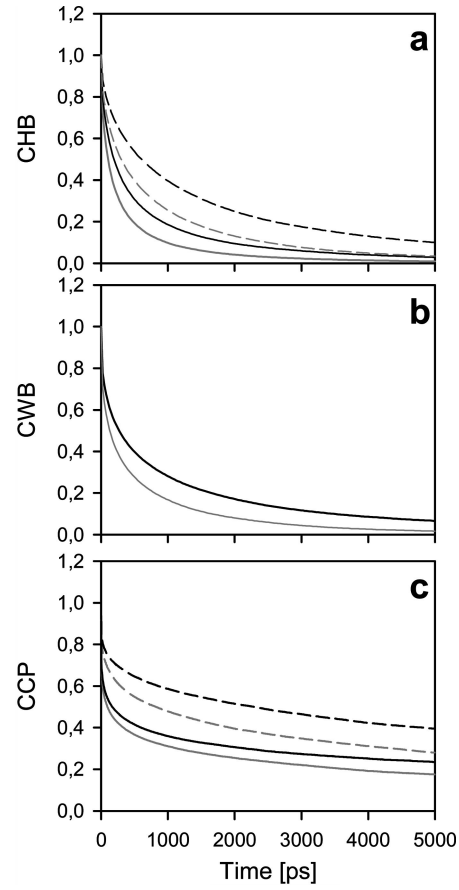

Figure 9. Time correlation functions for DPPC−water (a) H-bonds (C_{HB}), (b) water bridges (no distinction between oxygen atoms belonging to phosphate or carbonyl groups) (C_{WB}), and (c) charge pairs (C_{CP}) in DPPC−H_2O (gray line) and DPPC−D_2O (black line) bilayers. In (a) and (c), the solid line corresponds to the phosphate oxygen atoms (Op) and the broken line corresponds to the carbonyl oxygen atom O32.

exponentials provide the best and most consistent results. The corresponding values of A_i and T_i obtained by nonlinear fitting are given in Table 5.

Comparison of the curves in Figure 9 indicates that the probabilities of persistence of single D-bonds with DPPC headgroups and of water bridges involving D_2O molecules decay slower than the ones involving H_2O molecules. Additionally, the probability of persistence of water bridges and charge pairs decays slower when hydrating water is deuterated. The T_i and A_i values reported in Table 5 enable a more quantitative comparison of the decay rates of the postulated processes, which can be summarized as follows: (1) The T_1's for all processes (including charge pairs) in both systems are similar to each other and range between 2.5 and 4.1 ps. (2) The T_i's corresponding to Op−water H-bonds ($C^{Op}{}_{HB}$) in both bilayers are very similar to the T_i's corresponding to the PC−water bridges, C_{WB}, in these bilayers. (3) For both for $C^{Op}{}_{HB}$ and C_{WB}, the $T_i(D_2O)$ to $T_i(H_2O)$ ratios are ~2:1 except for T_1's. (4) For both systems, T_4's (the slowest decay) for $C^{Op}{}_{HB}$ and C_{WB} are very similar, but A_4 is twice as large for C_{WB} that for $C^{Op}{}_{HB}$. For A_2, the situation is reversed, whereas A_3 and T_3 are similar for $C^{Op}{}_{HB}$ and C_{WB}. These comparisons indicate that the lifetimes of single DPPC−water H (D)-bonds are almost the same as those of H_2O (D_2O) water bridges, but the number of long-lived water bridges is double that of single H (D)-bonds. This is consistent with quantum chemical calculations of Frischleder et al.,[41] who showed that the energy of a water bridge between two phosphate

TABLE 5: Multiexponential Nonlinear Fits to Time Correlation Functions[a]

function	A_1 D_2O/H_2O	T_1 D_2O/H_2O	A_2 D_2O/H_2O	T_2 D_2O/H_2O	A_3 D_2O/H_2O	T_3 D_2O/H_2O	A_4 D_2O/H_2O	T_4 D_2O/H_2O
C^{Op}_{HB}	20.6/23.2	4.1/3.1	40.0/39.0	44.6/26.5	31.0/30.2	201.7/109.8	8.3/7.6	887.0/481.0
C^{Oc}_{HB}	11.4/15.1	3.6/3.4	19.4/27.1	46.5/38.8	40.8/42.0	223.4/181.6	28.2/15.7	910.8/630.2
C_{WB}	22.2/26.5	3.0/2.5	25.4/26.6	38.9/26.2	34.5/30.8	213.9/128.3	17.9/16.2	955.8/444.3
C^{Op}_{CP}	32.3/34.2	2.7/2.6	16.0/17.0	85.8/69.4	17.1/16.7	707.7/554.5	34.5/32.1	12693.5/7977.4
C^{Oc}_{CP}	17.4/20.0	3.2/2.9	10.1/14.2	144.0/113.6	14.6/19.5	1112.5/844.9	56.9/46.3	13271.3/9937.8

[a] Amplitudes (A_i, %) and time constants (T_i, ps) of time correlation functions for Op−water (C^{Op}_{HB}) and O32−water (C^{Oc}_{HB}) H-bonds, water bridges (C_{WB}), and Op−choline (C^{Op}_{CP}) and O32−choline (C^{Oc}_{CP}) charge pairs, in DPPC−H_2O and DPPC−D_2O bilayers. Time correlation functions were fitted to a sum of four exponentials. Errors, estimated by the variance analysis, are not larger than 0.1% in the case of amplitudes and ∼1% in the case of time constants.

oxygen atoms is significantly lower than that of a single H-bond.[41] The lifetime of the long-lived water bridges in the DPPC−D_2O bilayer is ∼1 ns, to be compared with ∼0.5 ns in the case of the DPPC−H_2O bilayer. These water bridges constitute nearly 20% of all bridges in the bilayers. The remaining water bridges as well as H-bonds have much shorter lifetimes (Table 5 and Figure 9). The most persistent PC−PC interaction is charge pairing between the N−CH_3 group and Op or Oc; the lifetime of the long-lived component is over 1 order of magnitude longer than that of water bridges in the DPPC−D_2O bilayer.

Unambiguous interpretation of the lifetimes and amplitudes in Table 5 requires detailed additional studies at both quantum and atomistic scales. That is beyond the scope of this study, and work is in progress to address these issues in detail. At this point, we can only assess the elementary processes involved in the decay of the analyzed interactions. The membrane/water interface is a complex system, where motions of molecules and groups of atoms occur at different time scales. Therefore, relaxation of two molecules (PC···water) or groups (N−CH_3−Op(Oc)) from a bound to an unbound state involves different time scales. Let us next discuss these processes.

The largest contribution to the decay of PC−water H (D)-bonding is mobility due to water molecules (both translation and rotation) and the strength of the H (D)-bonding between DPPC and water molecules. Translational displacement of a H-bonded water molecule of less than 0.5 Å may lead to breaking of an H-bond. Such a displacement (cf. Figure 1 in refs 42 and 43), takes place within ∼2 ps and contributes to the short-lived decay component. If an H-bonded water molecule experiences angular reorientation of amplitude of more than 35°, the H-bond is broken. As the rotational correlation time of the interfacial water is in the range of 70−320 ps,[42] such reorientations contribute to the long-lived components of the decay. In addition, mobility of a water molecule has been shown to be lower near a carbonyl group than near a phosphate group.[42,43] Thus, the contribution of short-lived components is significantly higher to C^{Op}_{HB} than to C^{Oc}_{HB} in both bilayers.

The lifetimes of N−CH_3−Op charge pairs are affected by the relative mobility of both groups, whereas the lifetimes of N−CH_3−Oc charge pairs are affected by the mobility of N−CH_3 only. Importantly, time correlation functions also allow for temporal breaks which contribute to the long-lived components. In addition, formation of multiple H/D-bonds and charge pairs could lead to an increase of lifetimes.

Some elementary events contributing to the renewal processes in the H-bond network of water occur at femtosecond time scales. Currently, computer simulations provide the only method for investigations of such events; MD simulations of Laage and Hynes[44] demonstrate a new mechanism for renewal. They followed trajectories corresponding to H-bond reorientation toward a new acceptor and their subsequent new H-bonds (an H-bond switching event, HBSE). They observed this reorientation to be instantaneous with an angular amplitude of ∼60°. In order to achieve optimal proximity, translational motions of the old acceptor from the first hydration shell of the donor molecule away from particular oxygen, O*, and of the new acceptor away from the second hydration shell toward O*, occur.

Reorientation takes place when both acceptors are at equal distances from O* and the time scale is about 250 fs. At the interface of a biological entity, such as a protein, this rotation−translation coupling is perturbed;[45] translational motions of water molecules are constrained by their own H-bonds with hydrophilic sites and steric effects. As a result, within 4.25 Å from heavy atoms of the protein and near its hydrophilic sites, the forward rate constant of H-bond switching is reduced by 30% compared with bulk water. Moreover, in ∼80% of HBSE no translational motion of both acceptors occurs in 1 ps before or after the event: that particular hydroxyl, O*H*, rocks between the two acceptors. It may be postulated that similar evens occur at the interface of a phospholipid bilayer; in a bilayer system, the translational diffusion coefficient of water parallel to the interface is an order of magnitude smaller than in bulk water.[46]

The persistence of a particular H (D)-bond (HB*) between a site S and a particular water molecule W* is doubly favored with respect to the one of H (D)-bonds in the bulk waters. First, because of the relative immobility of S, the formation by W* of HB* with S is favored with respect to the formation of an H-bond with another water molecule. Second, as the only motions of W* are rocking between two acceptors, excluding any going out from the S hydration shell, the re-formation of HB* is favored.

Jana et al.[45] showed that when the translational motions of water molecules are constrained, their rotational motions have large angular amplitudes. In general, the expected isotope effect on diffusion of water due to the replacement of H by D varies with the type of motion. For translational motion, it is expected to be equal to $(m_{D_2O}/m_{H_2O})^{1/2} = 1.05$, whereas for rotational motion it is expected as equal to $(m_D/m_H)^{1/2} = 1.4$.[47] Consequently, reorientations with large angular amplitudes will be less frequent when water molecules are deuterated.

Let us now discuss a particular H (D)-bond (HB*) between a site S and a particular water molecule W*. As the frequency of large angle reorientations of W* is lower when W* is deuterated than when it is not, the persistence of HB* will be longer in the first case. Moreover, this isotope effect should appear beyond ∼10 ps, the delay corresponding to the emergence of these large angle reorientations. It is indeed what we have obtained. This interpretation is supported by Volkov et al.[15] ultrafast IR study on DMPC bilayers weakly hydrated by D_2O molecules. From their results, the lack of reorientation of these water molecules at 200 fs time scale can be inferred,

suggesting to us that HBSE are strongly inhibited.[15] Volkov et al., however, attributed this absence of reorientation of D_2O molecules only to the proximity of the DMPC bilayer. Our results suggest that they may rather result from the isotopic nature of water molecules.

In their bulk phases, transport properties in H_2O and D_2O differ. At 328 K the experimentally measured self-diffusion coefficients of normal and heavy water are equal to 4.46×10^{-5} and 3.54×10^{-5} cm^2/s, respectively.[38] They are smaller in our bilayer systems at the same temperature (2.58×10^{-5} cm^2/s for H_2O and 1.48×10^{-5} cm^2/s for D_2O, Table 2), and the corresponding isotope effect is larger (43% compared with 21% in the above experiments). This difference is not surprising as in our systems the number of water molecules per DPPC (28.5) is near the number of water molecules trapped in the interlamellar space of DPPC multibilayers in equilibrium at 50 °C (30[48]). The thickness of these interlamellar spaces is 20.5 Å for DPPC multibilayers at 50 °C. It is only twice the distance up to which the H-bond network of hydrating water is known to be perturbed by a phospholipid bilayer interface (10 Å[49]). At this interface water molecules are slowed down by their linkage to DPPC headgroups, which have a diffusion coefficient ~100 times smaller.[46]

In the case of two molecules (water and DPPC) in aqueous solutions, it has been evaluated that for equalizing their self-diffusion coefficients the duration of their linkage should be longer than ~10 ps[50]—a time much longer than the correlation time of the velocity correlation function of water (~0.1 ps). The characteristic time scale for the probability of persistence of D-bonds with DPPC headgroups differs from the corresponding one of H-bonds. This difference in duration of the linkage with DPPC headgroups amplifies the slowing down of D_2O molecules with respect to H_2O ones. Therefore, the large isotope effect of ~50% on the time-averaged self-diffusion coefficients of D_2O and H_2O molecules obtained in our systems may be assigned to the isotope effect on the probability of persistence of H (D)-bonds between these molecules and DPPC headgroups. In fact, in our systems all water molecules are influenced by the DPPC bilayer. Consequently, any local slowing down of water molecules will have repercussions on their global mobility.

Our results confirm that rotational and translational motions of water molecules are coupled. Thereby they provide an indirect support to the jump mechanism of Laage and Hynes.[44] It implies large angle reorientations of water molecules susceptible to the influence of isotope effect; it appears to be the only mechanism capable to interpret the rather large isotope effect on the self-diffusion coefficients of pure water.

Discussion

Water is essential to all known forms of life. It is of fundamental importance for the formation of folded protein structures and biomolecular assemblies and contributes to the structural, dynamic, and functional properties of all proteins and lipid bilayers (e.g., refs 51 and 52). To understand its role at the molecular and atomic levels, a large number of experimental (e.g., refs 3, 9, 51, and 53) and computational (e.g., refs 8, 13, 52, and 54) studies have been undertaken. The protein hydration studies indicate that water molecules that interact directly with atoms on the protein surface via H-bonds and vdW contacts (first-layer water[53]) form monolayer-like aggregates, where the water molecules are H-bonded to each other. The aggregates cover both hydrophobic and hydrophilic surface patches as well as flat surface areas and surface grooves of the protein and are anchored to the protein through H-bonds to polar groups at the protein surface.[55] Except for the water molecules that are tightly bound to the protein polar groups, hydration water molecules are mobile. They may move around the protein surface changing hydration sites or exchange with bulk water. Residence times of hydration water molecules at the hydration sites are broadly distributed and range from less than 5 ps to more than 100 ps.[56] Thus, water molecules form large-scale networks of H-bonds covering the surface of proteins. These networks are quite flexible to accommodate to the large-scale conformational changes of proteins.

A similar picture emerges from MD simulations[13] and experimental[57,58] studies of hydrated lipid bilayers. The recent review of Nagle and Tristram−Nagle indicates that in DPPC bilayers in the liquid-crystalline phase 8.6 water molecules are directly H-bonded to each DPPC molecule, but 30.1 water molecules are interacting with it.[48] Water molecules that are H-bonded to a PC were shown to cross-link neighboring PC molecules in the bilayer both in crystalline[59] and in liquid-crystalline[13] states. In the crystalline state, one-dimensional infinite PC−water ribbons are formed along a crystal axis. As evidenced by our previous studies,[13,14] PC cross-linking by water bridges in liquid-crystalline bilayers is less extended. Additionally, the average lifetime of an individual water bridge is ~50 ps in contrast to ~1 ns for PC—PC pairs bridged by water. This indicates that the recycling of bridging water molecules is slower than the corresponding ones implied in H-bonds.[14] Clathrate-like clusters of water molecules cover hydrophobic choline groups of PCs.[13] As demonstrated in this MD simulation study for the first time, these clathrates are anchored to PCs by water molecules (anchoring water, Table 3) forming a link between clathrates and polar groups.

In this study, we have compared selected properties of a DPPC bilayer hydrated by normal and heavy water as well as those of water molecules hydrating the bilayer. A simple SPC model for H_2O and SPC-HW for D_2O were used. In SPC-HW, the isotopic effect is modeled by twice-increased mass of the hydrogen atom and modified partial charges on the hydrogen and oxygen atoms, whereas the bonding and van der Waals parameters are the same as for H_2O.[18,19] In the case of pure water, the model correctly reproduces experimental data.[19] Our study shows the relevance and suitability of this D_2O model for studies of biomolecular aggregates by providing results that are fully consistent with experimental data. Exchange of H_2O by D_2O affects the time-averaged properties of the PC bilayer. When this bilayer is hydrated by D_2O molecules, in agreement with experimental results,[10] its core is more compact as its surface area is slightly decreased in comparison with the case in which it is hydrated by H_2O molecules (Table 2). This can be assigned to the more stable PC−water D- than H-bonds and, particularly, to the more stable network of D_2O water bridges compared with the H_2O ones as reflected by the higher density of the headgroup regions (Figure 3). This slight contraction of the surface area results in a denser packing of atoms in the center of the acyl chains (Figure 5), a higher degree of acyl chain order (Figure 4), and increased thickness (Table 2) of the DPPC bilayer when it is hydrated by D_2O molecules. The consequent less deep penetration of D_2O (than H_2O) into the bilayer core (Figure 3) might be the origin of the experimental observations by Tokutake et al.[11]

D_2O molecules are slightly better ordered than H_2O ones (Figure 7). This may result from more persistent PC−D_2O bonds and smaller mobility (both translational and rotational) of D_2O relative to H_2O. More importantly, the self-diffusion coefficient averaged over all water molecules in the bilayer is almost twice

smaller than that of H_2O (Table 2 and Figure 8) and ~2.5 times smaller than in pure D_2O (~1.7 in the case of H_2O).[38] This results from more stable single PC−water D-bonds and D_2O water bridges than the corresponding ones with H_2O molecules. Indeed, analysis based on time correlation functions (Figure 9a,b and Table 5) indicates that the renewal of water molecules implied in water bridging or single H (D)-bonds is much slower when these molecules are deuterated than they are not. This analysis also indicates that the stability of charge pairs is higher in the DPPC−D_2O than DPPC−H_2O bilayer (Figure 9c and Table 5). These results lead to the conclusion that in the DPPC bilayer hydrated with D_2O not only the PC−PC interactions involving water are more persistent but also the electrostatic interactions. In general, the lifetime of charge pairs is longer than that of hydrogen bonds and water bridges.[15] This, most likely, results from ~100 times slower relative motions of fragments of PC molecules compared to mobility of water molecules.

Let us finish this discussion by looking at the number of water molecules H-bonded to the carbonyl oxygen atom O22. Here, the number is ~1.5 and is much larger than ~0.6 which we obtained in our previous MD simulation studies.[13,14,61] In those studies, we used the AMBER 5.0 program package[62] and OPLS (Optimized Parameters for Liquid Simulations) parameters for lipids[63] and TIP3P (Transferable Intermolecular Potential 3-Point) parameters for water.[64] The current study was carried out on a bilayer (DPPC−H_2O) that was the final structure of the DPPC bilayer simulated for 100 ns using the GROMACS software package[21] and characterized in ref 20. For the bilayer, a much larger number of water molecules H-bonded to O22 than O32 of DPPC was demonstrated by Niemelä et al. in ref 65 (see also the Supporting Information in ref 65). In the present study, the DPPC−D_2O bilayer was generated by substituting of D_2O for H_2O in the DPPC−H_2O bilayer. Both bilayers were MD simulated for over 50 ns using the GROMACS software package,[21] the same force-field parameters, and the same simulation protocol as in refs 20 and 65, however different than those used in refs 13, 14, and 61. Here, as well as in our previous studies, we used the SPC water model. Quantum mechanical calculations using the SPC model potential have been recently compared to high-precision synchrotron radiation experiments for H_2O and D_2O and were shown to compare surprisingly well.[66] That provides further validation of the present results. Although a classical model misses quantum effects, especially the inclusion of zero-point energy level, which increases the dipole moment,[67] the SPC model seems a reasonable approximation of the real system.

Conclusions

There are only small differences in the time-averaged properties of the DPPC−H_2O and DPPC−D_2O bilayers (Tables 2−4, except the diffusion coefficients), whereas time-dependent properties of these bilayers differ significantly. The large differences in the latter relate mainly to the stability of PC−water and PC−PC interactions reflected by the decays of the time correlation function (Figure 9 and Table 5) and by the self-diffusion coefficient of bilayer water (Table 2, last entry). These isotope effects reveal the importance of the dynamics of phospholipid bilayers and the role of the network of PC−PC links via water bridges.

As the mobility of water molecules near the interface of a phospholipid bilayer depends on its isotopic nature, it can be postulated that the mobility of phospholipid molecules in this bilayer also depends on the isotopic nature of hydrating water. The correlations between dynamical properties of hydrating water (lifetimes of H-bonds, rotational and translational diffusion, and re-formation dynamics of H-bonding network) and properties of a phospholipid bilayer warrant a separate detailed study which is currently being undertaken.

The results of our calculations emphasize the dynamic character of the interactions between phospholipid bilayers and hydrating water molecules. When replacing H_2O molecules by D_2O, the time-averaged number of H (D)-bonds changes only slightly. In contrast, the time-resolved persistence of these H (D)-bonds strongly depends on the isotopic nature of water. In particular, isotope effect on persistence of water bridges may have important consequences as it affects compactness and flexibility of phospholipid bilayers as revealed in recent experiments. Changing the isotopic composition of water in DPPC/water/pyridine reverse micelles has been shown by SANS to change drastically the stiffness of the DPPC monolayer enveloping these micelles.[39]

Finally, the water isotope effects revealed by our results question the validity of the procedure of substituting of H_2O by D_2O as solvent in numerous spectroscopic methods.

Acknowledgment. This work was partly supported by the Academy of Finland and the Natural Science and Engineering Research Council (NSERC) of Canada (M.K.). Computational resources were provided by the Finnish IT Center for Science (CSC), the SharcNet (www.sharcnet.ca) computing facility, and the HorseShoe supercluster at the University of Southern Denmark. T.R. holds a Marie Curie Intra-European Fellowship "024612-Glychol". K.M. acknowledges a fellowship award from Adam Krzyżanowski Foundation, Jagiellonian University, Poland. We thank Michał Markiewicz for his help in curve fitting.

References and Notes

(1) Guillot, B. A reappraisal of what we have learnt during three decades of computer simulations on water. *J. Mol. Liq.* **2002**, *101*, 219–260.

(2) Cioni, P.; Strambini, G. B. Effect of heavy water on protein flexibility. *Biophys. J.* **2002**, *82*, 3246–3253.

(3) Sasisanker, P.; Oleinikova, A.; Weingärtner, H.; Ravindra, R.; Winter, R. Solvation properties and stability of ribonuclease A in normal and deuterated water studied by dielectric relaxation and differential scanning/pressure perturbation calorimetry. *Phys. Chem. Chem. Phys.* **2004**, *6*, 1899–1905.

(4) Kushner, D. J.; Baker, A.; Dunstall, T. G. Pharmacological uses and perspectives of heavy water and deuterated compounds. *Can. J. Physiol. Pharmacol.* **1999**, *77*, 79–88.

(5) Litvineko, L. A.; Kravchuk, A. V.; Petrikevich, S. B.; Sakharovskii, V. G.; Ivanitskaya, Y. G.; Gulyamova, D. E. Effect of heavy-water on the growth and glucose assimilation by *Escherichia coli*, and on its resistance to freeze-thawing. *Microbiology* **1992**, *61*, 725–730.

(6) Newo, A. N. S.; Pshenichnikova, A. B.; Skladnev, D. A.; Shvets, V. I. Deuterium oxide as a stress factor for the methylotrophic bacterium *Methylophilus* sp B-7741. *Microbiology* **2004**, *73*, 139–142.

(7) Scheiner, S.; Cuma, M. Relative stability of hydrogen and deuterium bonds. *J. Am. Chem. Soc.* **1996**, *118*, 1511–1521.

(8) Berkowitz, M. L.; Bostick, D. L.; Pandit, S. Aqueous solutions next to phospholipid membrane surfaces: insights from simulations. *Chem. Rev.* **2006**, *106*, 1527–1539.

(9) Milhaud, J. New insights into water-phospholipid model membrane interactions. *Biochim. Biophys. Acta* **2004**, *1663*, 19–51.

(10) Matsuki, H.; Okuno, H.; Sakano, F.; Kusube, M.; Kaneshina, S. Effect of deuterium oxide on the thermodynamic quantities associated with phase transitions of phosphatidylcholine bilayer membranes. *Biochim. Biophys. Acta* **2005**, *1712*, 92–100.

(11) Tokutake, N.; Jing, B.; Regen, S. L. Probing the hydration of lipid bilayers using a solvent isotope effect on phospholipid mixing. *Langmuir* **2004**, *20*, 8958–8960.

(12) Milhaud, J.; Hantz, E.; Liquier, J. Different properties of H_2O- and D_2O-containing phospholipid-based reverse micelles near a critical temperature. *Langmuir* **2006**, *22*, 6068–6077.

(13) Pasenkiewicz-Gierula, M.; Takaoka, Y.; Miyagawa, H.; Kitamura, K.; Kusumi, A. Hydrogen bonding of water to phosphatidylcholine in the

membrane as studied by a molecular dynamics simulation: location, geometry, and lipid-lipid bridging via hydrogen-bonded water. *J. Phys. Chem. A* **1997**, *101*, 3677–3691.

(14) Pasenkiewicz-Gierula, M.; Takaoka, Y.; Miyagawa, H.; Kitamura, K.; Kusumi, A. Charge pairing of headgroups in phosphatidylcholine membranes: a molecular dynamics simulation study. *Biophys. J.* **1999**, *76*, 1228–1240.

(15) Volkov, V. V.; Palmer, D. J.; Righini, R. Heterogeneity of water at the phospholipid membrane interface. *J. Phys. Chem. B* **2007**, *111*, 1377–1383.

(16) Lawrence, C. P.; Skinner, J. L. Flexible TIP4P model for molecular dynamics simulation of liquid water. *Chem. Phys. Lett.* **2003**, *372*, 842–847.

(17) Guzzi, R.; Arcangeli, C.; Bizzarri, A. R. A molecular dynamics simulation study of the solvent isotope effect on copper plastocyanin. *Biophys. Chem.* **1999**, *82*, 9–22.

(18) Campo, M. G.; Grigera, J. R. Molecular dynamics simulation of OH^- in water. *Mol. Simul.* **2004**, *30*, 537–542.

(19) Grigera, J. R. An effective pair potential for heavy water. *J. Chem. Phys.* **2001**, *114*, 8064–8067.

(20) Vainio, S.; Jansen, M.; Koivusalo, M.; Róg, T.; Karttunen, M.; Vattulainen, I.; Ikonen, E. Desmosterol cannot replace cholesterol in lipid rafts. *J. Biol. Chem.* **2006**, *281*, 348–355.

(21) Lindahl, E.; Hess, B.; van der Spoel, D. GROMACS 3.0: a package for molecular simulation and trajectory analysis. *J. Mol. Model.* **2001**, *7*, 306–317.

(22) Berger, O.; Edholm, O.; Jahnig, F. Molecular dynamics simulations of a fluid bilayer of dipalmitoylphosphatidylcholine at full hydration, constant pressure, and constant temperature. *Biophys. J.* **1997**, *72*, 2002–2013.

(23) Tieleman, D. P.; Berendsen, H. J. C. Molecular dynamics simulations of a fully hydrated dipalmitoylphosphatidylcholine bilayer with different macroscopic boundary conditions and parameters. *J. Chem. Phys.* **1996**, *105*, 4871–4880.

(24) Berendsen, H. J. C.; Postma, J. P. M.; van Gunsteren, W. F.; Hermans, J. Interaction models for water in relation to protein hydration. In *Intermolecular Forces*; Pullman, B., Ed.; Reidel: Dordrecht, The Netherlands, 1981.

(25) Hess, B.; Bekker, H.; Berendsen, H. J. C.; Fraaije, J. G. E. M. LINCS: a linear constraint solver for molecular simulations. *J. Comput. Chem.* **1997**, *18*, 1463–1472.

(26) Essmann, U.; Perera, L.; Berkowitz, M. L.; Darden, T.; Lee, H.; Pedersen, L. G. A smooth particle mesh Ewald method. *J. Chem. Phys.* **1995**, *103*, 8577–8592.

(27) Patra, M.; Karttunen, M.; Hyvönen, M. T.; Falck, E.; Vattulainen, I. Lipid bilayers driven to a wrong lane in molecular dynamics simulations by truncation of long-range electrostatic interactions. *J. Phys. Chem. B* **2004**, *108*, 4485–4494.

(28) Vist, M. R.; Davis, J. H. Phase equilibria of cholesterol/dipalmitoylphosphatidyl-choline mixtures: ^2H nuclear magnetic resonance and differential scanning calorimetry. *Biochemistry* **1990**, *29*, 451–464.

(29) Berendsen, H. J. C.; Postma, J. P. M.; van Gunsteren, W. F.; DiNola, A.; Haak, J. R. Molecular dynamics with coupling to an external bath. *J. Chem. Phys.* **1984**, *81*, 3684–3690.

(30) Patra, M.; Salonen, E.; Terama, E.; Vattulainen, I.; Faller, R.; Lee, B. W.; Holopainen, J.; Karttunen, M. Under the influence of alcohol: the effect of ethanol and methanol on lipid bilayers. *Biophys. J.* **2006**, *90*, 1121–1135.

(31) Róg, T.; Pasenkiewicz-Gierula, M. Cholesterol effects on the phosphatidylcholine bilayer nonpolar region: a molecular simulation study. *Biophys. J.* **2001**, *81*, 2190–2202.

(32) Róg, T.; Gurbiel, R.; Takaoka, Y.; Kusumi, A.; Pasenkiewicz-Gierula, M. Effects of phospholipid unsaturation on the bilayer nonpolar region: a molecular dynamics study. *J. Lipid Res.* **2004**, *45*, 326–336.

(33) Hubbell, W. L.; McConnell, H. M. Molecular motion in spin-labeled phospholipids and membranes. *J. Am. Chem. Soc.* **1971**, *93*, 314–326.

(34) Heller, H.; Schaefer, M.; Schulten, K. Molecular dynamics simulation of a bilayer of 200 lipids in the gel and liquid-crystal phases. *J. Phys. Chem.* **1993**, *97*, 8343–8360.

(35) Róg, T.; Pasenkiewicz-Gierula, M. Cholesterol effects on the membrane packing and condensation: a molecular simulation study. *FEBS Lett.* **2001**, *502*, 68–71.

(36) Róg, T.; Pasenkiewicz-Gierula, M. Non-polar interactions between cholesterol and phospholipids: a molecular dynamics simulation study. *Biophys. Chem.* **2004**, *107*, 151–164.

(37) Nemethy, G.; Scheraga, H. Structure of water and hydrophobic bonding in proteins. IV. The thermodynamic properties of liquid deuterium oxide. *J. Chem. Phys.* **1964**, *41*, 680–689.

(38) Woolf, L. A. Tracer diffusion of tritiated heavy water (DTO) in heavy water (D_2O) under pressure. *J. Chem. Soc., Faraday Trans. 1* **1976**, 1267–1273.

(39) Balasubramanian, S.; Pal, S.; Bagchi, B. Hydrogen-bond dynamics near a micellar surface: origin of the universal slow relaxation at complex aqueous interfaces. *Phys. Rev. Lett.* **2002**, *89*, 115505−1115505−4.

(40) Istratov, A. A.; F Vyvenko, O. Exponential analysis in physical phenomena. *Rev. Sci. Instrum.* **1999**, *70*, 1233–1257.

(41) Frischleder, H.; Gleichmann, S.; Krahl, R. Quantum-chemical and empirical calculations on phospholipids. III. Hydration of the dimethylphosphate anion. *Chem. Phys. Lipids* **1977**, *19*, 144–149.

(42) Róg, T.; Murzyn, K.; Pasenkiewicz-Gierula, M. The dynamics of water at the phospholipid bilayer surface: a molecular dynamics simulation study. *Chem. Phys. Lett.* **2002**, *352*, 323–327.

(43) Murzyn, K.; Zhao, W.; Karttunen, M.; Kurdziel, M.; Róg, T. Dynamics of water at membrane surfaces: Effect of headgroup structure. *Biointerphases* **2006**, *1*, 98–105.

(44) Laage, D. A molecular jump mechanism of water reorientation. *Science* **2006**, *311*, 832–835.

(45) Jana, B.; Pal, S.; Bagchi, B. Hydrogen bond breaking mechanism and water reorientational dynamics in the hydration layer of lysozyme. *J. Phys. Chem. B* **2008**, *112*, 9112–9117.

(46) Wassal, S. R. Pulsed field gradient-spin echo NMR studies of water diffusion in a phospholipid model membrane. *Biophys. J.* **1996**, *71*, 2724–2732.

(47) Agmon, N. 1996. Tetrahedral displacement: the molecular mechanism behind the Debye relaxation in water. *J. Phys. Chem.* **1996**, *100*, 1072.

(48) Nagle, J. F.; Tristram-Nagle, S. Structure of Lipid Bilayers. *Biochim. Biophys. Acta* **2000**, *1469*, 159–195.

(49) Marrink, S. J.; Berkowitz, M.; Berendsen, H. J. C. Molecular dynamics simulation of a membrane water interface: the ordering of water and its relation to the hydration force. *Langmuir* **1993**, *9*, 3122–3131.

(50) Hertz, H. G. In *Water: A Comprehensive Treatise*; Franks, F., Ed.; Plenum Press: New York, Vol. 3, p 301, 1973.

(51) Chaplin, M. Do we underestimate the importance of water in cell biology. *Nat. Rev. Mol. Biol.* **2006**, *7*, 861–866.

(52) Dias, C. L.; Ala-Nissila, T.; Karttunen, M.; Vattulainen, I.; Grant, M. Microscopic mechanism for cold denaturation. *Phys. Rev. Lett.* **2008**, *100*, 118101.

(53) Nakasako, M. Water—protein interactions from high-resolution protein crystallography. *Philos. Trans. R. Soc. London B* **2004**, *359*, 1191–1206.

(54) Fischer, S.; Verma, C. S.; Hubbard, R. E. Rotation of structural water inside a protein: calculation of the rate and vibrational entropy of activation. *J. Phys. Chem. B* **1998**, *102*, 1797–1805.

(55) Nakasako, M. Large-scale networks of hydration water molecules around bovine β-trypsin revealed by cryogenic X-ray crystal structure analysis. *J. Mol. Biol.* **1999**, *289*, 547–564.

(56) Higo, J.; Nakasako, M. Hydration structure of human lysozyme investigated by molecular dynamics simulation and cryogenic X-ray crystal structure analyses: on the correlation between crystal water sites, solvent density, and solvent dipole. *J. Comput. Chem.* **2002**, *23*, 1323–1336.

(57) Gawrisch, K.; Arnold, K.; Gottwald, T.; Klose, G.; Volke, F. ^2D NMR studies of the phosphate-water interaction in dipalmitoylphosphatidylcholine-water system. *Stud. Biophys.* **1978**, *74*, 13–14.

(58) Nagle, J. F. Area/lipid of bilayers from NMR. *Biophys. J.* **1993**, *64*, 1476–1481.

(59) Pearson, R. H.; Pascher, I. The molecular structure of Lecithin dihydrate. *Nature (London)* **1979**, *281*, 499–501.

(60) Vidulich, G. A.; Evans, D. F.; Kay, R. L. The dielectric constant of water and heavy water between 0 and 40°. *J. Phys. Chem.* **1967**, *71*, 656–662.

(61) Murzyn, K.; Róg, T.; Jezierski, G.; Takaoka, Y.; Pasenkiewicz-Gierula, M. Effects of phospholipid unsaturation on the membrane/water interface: a molecular simulation study. *Biophys. J.* **2001**, *81*, 170–183.

(62) Case, D. A.; Pearlman, D. A.; Caldwell, J. W.; Cheatham, T. E., III; Ross, W. S.; Simmerling, C.; Darden, T. A.; Merz, K. M.; Stanton, R. V.; Cheng, A. L.; Vincent, J. J.; Crowley, M.; Ferguson, D. M.; Radmer, R. J.; Seibel, G. L.; Singh, U. C.; Weiner, P. K.; Kollman, P. A. AMBER 5.0, University of California, San Francisco, 1997.

(63) Jorgensen, W. L.; Tirado-Rives, J. The OPLS potential functions for proteins: energy minimization for crystals of cyclic peptides and crambin. *J. Am. Chem. Soc.* **1988**, *110*, 1657–1666.

(64) Jorgensen, W. L.; Chandrasekhar, J.; Madura, J. D.; Impey, R. W.; Klein, M. L. Comparison of simple potential functions for simulating liquid water. *J. Chem. Phys.* **1983**, *79*, 926–935.

(65) Niemela, P.; Hyvönen, M. T.; Vattulainen, I. Structure and dynamics of sphingomyelin bilayer: insight gained through systematic comparison to phosphatidylcholine. *Biophys. J.* **2004**, *87*, 2976–2989 (Supplemental Material).

(66) Tomberli, B.; Benmore, C. J.; Egelstaff, P. A.; Neuefeind, J.; Honkimäki, V. Isotopic quantum effects in water structure measured with high energy photon diffraction. *J. Phys.: Condens. Matter* **2000**, *12*, 2597–2612.

(67) Chen, B.; Ivanov, I.; Klein, M. L.; Parrinello, M. Hydrogen bonding in water. *Phys. Rev. Lett.* **2003**, *91*, 215503.

JP8048235